

First-principles calculations of solute-vacancy interactions in aluminum

Sha-Sha Zhang(张莎莎), Zheng-Jun Yao(姚正军), Xiang-Shan Kong(孔祥山), Liang Chen(陈良), Jing-Yu Qin(秦敬玉)

Citation: Chin. Phys. B . 2020, 29(6): 066103 . **doi:** 10.1088/1674-1056/ab8458
Journal homepage: http://cpb.iphy.ac.cn; http://iopscience.iop.org/cpb

What follows is a list of articles you may be interested in

Electronic and optical properties of GaN-MoS_2 heterostructure from first-principles calculations

Dahua Ren(任达华), Xingyi Tan(谭兴毅), Teng Zhang(张腾), Yuan Zhang(张源)

Chin. Phys. B . 2019, 28(8): 086104 . **doi:** 10.1088/1674-1056/28/8/086104

Structural, magnetic properties, and electronic structure of hexagonal FeCoSn compound

Yong Li(李勇), Xue-Fang Dai(代学芳), Guo-Dong Liu(刘国栋), Zhi-Yang Wei(魏志阳), En-Ke Liu(刘恩克), Xiao-Lei Han(韩小磊), Zhi-Wei Du(杜志伟), Xue-Kui Xi(郗学奎), Wen-Hong Wang(王文洪), Guang-Heng Wu(吴光恒)

Chin. Phys. B . 2018, 27(2): 026101 . **doi:** 10.1088/1674-1056/27/2/026101

Segregation of alloying atoms at a tilt symmetric grain boundary in tungsten and their strengthening and embrittling effects

Li Zhi-Wu, Kong Xiang-Shan, Liu-Wei, Liu Chang-Song, Fang Qian-Feng

Chin. Phys. B . 2014, 23(10): 106107 . **doi:** 10.1088/1674-1056/23/10/106107

Structural stability and electronic properties of carbon star lattice monolayer

Fan Xue-Lan, Niu Chun-Yao, Wang Xin-Quan, Wang Jian-Tao, Li Han-Dong

Chin. Phys. B . 2014, 23(9): 096104 . **doi:** 10.1088/1674-1056/23/9/096104

Ground-state structure determination and mechanical properties of palladium seminitride

Zhang Gang-Tai, Bai Ting-Ting, Zhao Ya-Ru, Lu Cheng

Chin. Phys. B . 2013, 22(11): 116104 . **doi:** 10.1088/1674-1056/22/11/116104

First-principles calculations of solute–vacancy interactions in aluminum*

Sha-Sha Zhang(张莎莎)[1,†], Zheng-Jun Yao(姚正军)[1], Xiang-Shan Kong(孔祥山)[2,‡], Liang Chen(陈良)[2], and Jing-Yu Qin(秦敬玉)[2]

[1] College of Materials and Technology, Nanjing University of Aeronautics and Astronautics, Nanjing 211106, China
[2] Key Laboratory for Liquid–Solid Structural Evolution and Processing of Materials, Ministry of Education, Shandong University, Jinan 250061, China

(Received 3 March 2020; revised manuscript received 25 March 2020; accepted manuscript online 30 March 2020)

The interactions of solute atoms with vacancies play a key role in diffusion and precipitation of alloying elements, ultimately influencing the mechanical properties of aluminum alloys. In this study, first-principles calculations are systematically performed to quantify the solute–vacancy interactions for the 3d–4p series and the 4d–5p series. The solute–vacancy interaction gradually transforms from repulsion to attraction from left to right. The solute–vacancy binding energy is sensitive to the supercell size for elements at the beginning. These behaviors of the solute–vacancy binding energy can be understood in terms of the combination and competition between the elastic and electronic interactions. Overall, the electronic binding energy follows a similar trend to the total binding energy and plays a major role in the solute–vacancy interactions.

Keywords: first-principles calculations, solute–vacancy binding, aluminum alloys

PACS: 61.72.jd, 81.05.Bx, 63.20.dk, 71.55.−i **DOI:** 10.1088/1674-1056/ab8458

1. Introduction

Due to high specific strength, good abrasion, corrosion, and impact resistance, aluminum and its alloys are widely used in various areas such as aerospace and automobile industries.[1] To satisfy the requirements for the mechanical properties, the aluminum alloys are primarily strengthened by aging hardening with the addition of alloying elements. The interaction between vacancies and solute atoms is a key factor in understanding the basic physical processes, such as diffusion of solutes and other species, segregation, ordering, *etc*. Those processes are of significance for the aging hardening behavior. Moreover, the elucidation of the origin for the solute–vacancy (hereafter, a vacancy is denoted by □) interactions is indispensable for designing the future high strength or new performance aluminum alloys. The energetic bindings between the vacancies and the solute atoms have been widely studied experimentally[2–6] and theoretically.[7–9] However, there exist some discrepancies in the reported experimental values due to the different techniques utilized and the reliabilities of the measurements. The difference in the calculation methods and parameters gives rise to the discrepancy in theoretical solute–□ binding energy. Moreover, it is still not clear how the physical factors control the solute–vacancy interactions.

Generally, the solute-point defect interactions are governed by two primary factors, *i.e*., the electronic effect and the strain-relief effect. The effect of electronic structure and atomic distortion on the solute–□ interaction have been widely investigated in Fe,[10,11] W,[12] and Mg.[13] However, the role of electronic structure and the solute size in controlling the solute–□ interactions has not been fully unraveled in aluminum. Hoshino *et al.* understood the repulsive interaction of a vacancy with 3d and 4d impurities by the breakup of the strong sp–d bonds whereas the attractive interaction might be attributed to the energy gain due to the formation of stronger sp–sp bond.[9] Wolverton studied the dependence of solute–□ binding energy on solute size for the widely used 24 kinds of solutes in aluminum and found the close correlation between binding energy and the solute size for each of Cd, In, Sn, Sb, Pb, and Bi.[7] However, the effects of solute size on binding energy for other elements are still unclear. The role of electronic interaction in the solute–□ interactions was not taken into account.

In the present study, we carry out systematic first-principles calculations to investigate the binding energy values between the 3d, 4p, 4d, 5p solutes and the vacancies in aluminum, which are further decomposed into distortion and electronic binding energy in order to clarify the dominant physical factors that control the solute–□ interactions.

*Project supported by the National Natural Science Foundation of China (Grant Nos. 51701095 and 51771185) and the Natural Science Foundation of Jiangsu Province, China (Grant No. BK20170798).

†Corresponding author. E-mail: s.zhang@nuaa.edu.cn
‡Corresponding author. E-mail: xskong@sdu.edu.cn

© 2020 Chinese Physical Society and IOP Publishing Ltd

2. Calculation methods

First-principles calculations were performed within the framework of density functional theory (DFT) with the generalized gradient approximation (GGA) of Perdew–Burke–Ernzerhof (PBE) type[14] by using the Vienna *ab initio* simulation package (VASP).[15,16] The interactions between the ions and valence electrons were described by the projector augmented wave (PAW) method.[17,18] A supercell in a face-centered cubic (fcc) structure was built with $3\times3\times3$ unit cells, composed of 108 lattice sites. The Brillouin zone was sampled by the Monkhorst–Pack scheme with a $6\times6\times6$ k-point mesh.[19] A plane wave cutoff of 400 eV was used. The relaxations of atomic position and optimizations of the shape and size of the supercell were implemented. The structural optimization was truncated when the forces converge to less than 0.01 $e/$Å.

The vacancy formation energy $E_{\rm f}^{\square}$ is calculated by the following equation:

$$E_{\rm f}^{\square}=E_{\rm tot}^{\square}-\frac{107}{108}E_{\rm tot}^{\rm bulk}, \tag{1}$$

where $E_{\rm tot}^{\square}$ is the total energy of the supercell containing one vacancy, and $E_{\rm tot}^{\rm bulk}$ is the total energy of the perfect Al bulk.

The binding energy of the vacancy and solute is defined as

$$E_{\rm b}^{{\rm Sol}-\square}=E_{\rm tot}^{\rm Sol}+E_{\rm tot}^{\square}-E_{\rm tot}^{{\rm Sol}+\square}-E_{\rm tot}^{\rm bulk}, \tag{2}$$

where $E_{\rm tot}^{{\rm Sol}+\square}$ is the total energy of the supercell containing a solute atom and a vacancy and $E_{\rm tot}^{\rm Sol}$ is the total energy of the supercell containing a solute atom. In this paper, only nearest-neighbor (NN) binding between the vacancy and the solute is considered. Figure 1 displays the solute–vacancy configuration in the fcc Al matrix.

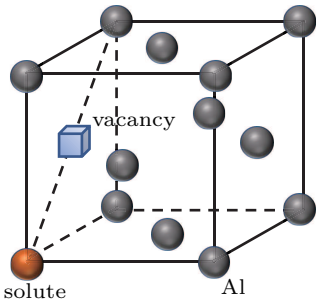


Fig. 1. Schematic diagram of solute–vacancy configuration in fcc Al.

3. Results

3.1. Validation of calculations

To verify our first-principles calculations, we investigate some fundamental properties of Al by calculating the lattice constant, bulk modulus, and vacancy formation energy. In addition, the binding energy between solutes Mg, Si, and the vacancy ($E_{\rm b}^{{\rm Mg}-\square}$ and $E_{\rm b}^{{\rm Si}-\square}$) are also calculated since Mg and Si are the common alloying elements in Al and have been extensively investigated previously. All calculated results are listed in Table 1 and compared with the reported experimental[6,20–22] and theoretical data.[7,8,23–25] As shown in Table 1, our calculated results are consistent with the previous theoretical results, and the theoretical values are in good agreement with the corresponding experimental data. The comparisons prove the accuracy and validity of the present first-principles calculations.

Table 1. Fundamental properties of Al. Lattice constant a, bulk modulus B, vacancy formation energy $E_{\rm f}^{\square}$, binding energies Mg–□ and Si–□.

Method	a/Å	B/Mbar	$E_{\rm f}^{\square}$/eV	Mg–□/eV	Si–□/eV
Expt	4.03[20]	0.77[21]	0.73 ± 0.04[22]	0.01 ± 0.04[6]	0.03[6]
DFT-LDA	3.983,[23] 3.961[24]	0.840,[23] 0.830[24]	0.70[25]	−0.02[7]	
DFT-GGA	4.039,[23] 4.042[24]	0.773,[23] 0.744[24]	0.75[8]	0.01[8]	0.08,[7] 0.05[8]
This work	4.040	0.778	0.73	0.00	0.06

3.2. Solute–vacancy binding energy of 3d, 4p, 4d, 5p elements

Figure 2 shows the variations of binding energy of solutes with vacancies for 3d, 4p, 4d, 5p solutes with atomic number. Positive energy means the attractive interaction while negative energy refers to the repulsion. For the 3d and 4p row (Fig. 2(a)), the solute–□ interaction gradually transforms from repulsion to attraction from left to right. The element Ti shows the maximum repulsive binding energy (−0.20 eV) whereas the element As has the maximum attraction interaction (0.19 eV) with the vacancy. The binding energy values between the solutes and vacancies are small in the middle of this series. For the 4d and 5p series (Fig. 2(b)), a similar evolution is observed, *i.e.*, at the beginning the interaction is repulsive and in the end the binding force is attractive. The elements Nb and Sb demonstrate the maximum repulsion and attraction with the vacancy, corresponding to their binding energy of −0.22 eV and 0.30 eV, respectively. For comparison, the calculated solute–□ binding energy values from Refs. [7,8] are also included. The evolution of the binding energy demonstrates the same trend as the reported results.

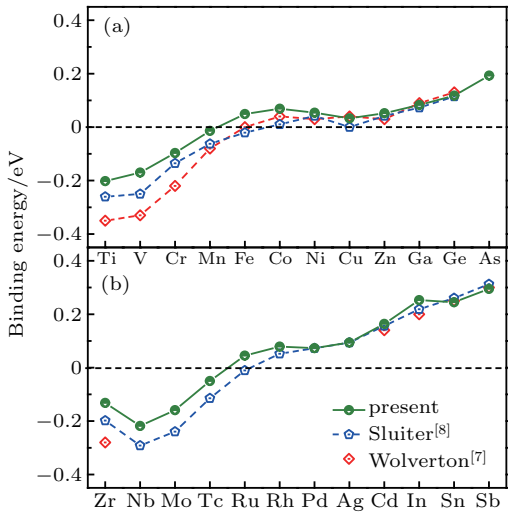


Fig. 2. Variations of solute–□ binding energy of (a) 3d and 4p, and (b) 4d and 5p elements in fcc Al with atomic number. Other DFT results from Refs. [7,8] are also included.

It is worth noting that for the 3d–4p and 4d–5p series the energy values for the late elements are impressively the same while there exist noticeable discrepancies for the elements in the beginning. The repulsive reactions are lower than those estimated by Simonovic and Sluiter,[8] whereas the repulsive bindings are highest in the work from Wolverton.[7] Simonovic and Sluiter have reproduced Wolverton's results by changing the number of k-points.[8] Comparing the calculation parameters with the previous results,[7,8] we find that a dominant discrepancy originates from the supercell size. The 108-atom supercell is utilized in the present study whereas the supercell containing 64 atoms has been built in the published work. Here, the supercells with different sizes are also used to calculate the binding energy of Ti, V, and Zr, as well as Ge and Sn for comparison.

As shown in Table 2, our results calculated by 64-atom supercell show high consistency with Wolverton's. It seems that for the early elements, a large supercell is essential. The interesting point is that the discrepancy within the supercell size gives essentially no change for Ge nor Sn.

Table 2. Comparison of solute–□ binding energy values (in units of eV) for Ti, V, Zr, Ge, Sn between supercell sizes containing 64 atoms and 108 atoms.

	Solute element					Supercell	Exchange	Energy	k-points
	Ti	V	Zr	Ge	Sn	size/atoms	correlation	cutoff/eV	
This work	0.20	0.17	0.13	0.12	0.25	108	GGA–PBE	400	$6\times6\times6$
This work	0.33	0.34	0.28	0.11	0.25	64	GGA–PBE	400	$6\times6\times6$
Wolverton[7]	0.35	0.33	0.28		0.25	64	LDA–PW91	237	$24\times24\times24$
Wolverton[7]				0.13		64	GGA–PW91	237	$24\times24\times24$
Sluiter[8]	0.26	0.25	0.20	0.12	0.26	64	GGA–PBE	300	$7\times7\times7$

3.3. Physics behind solute–□ binding energy

Generally, the solute–□ interaction is mainly ascribed to the elastic and electronic interactions. In this way, the total binding energy can be decomposed into elastic binding energy $E_{\rm b}^{\rm d}$ and electronic binding energy $E_{\rm b}^{\rm e}$,[12] *i.e.*,

$$E_{\rm b}^{\rm Sol-\square} = E_{\rm b}^{\rm d} + E_{\rm b}^{\rm e}. \tag{3}$$

The elastic binding energy is defined as

$$E_{\rm b}^{\rm d} = E_{\rm tot}^{\rm Sol}({\rm Al}) + E_{\rm tot}^{\square} - E_{\rm tot}^{\rm Sol+\square}({\rm Al}) - E_{\rm tot}^{\rm bulk}, \tag{4}$$

where $E_{\rm tot}^{\rm Sol}({\rm Al})$ and $E_{\rm tot}^{\rm Sol+\square}({\rm Al})$ are the energy of supercells when the solute atom is removed from the fully relaxed supercell containing a solute atom and solute–□ pair, respectively. $E_{\rm b}^{\rm e}$ can be calculated from Eq. (3).

Firstly, to reveal the effect of supercell size on the elastic and electronic interactions, we further calculate the elastic binding energy and electronic binding energy of solutes Ti, V, Zr, Ge, and Sn in the case of 108-atom and 64-atom supercells. As shown in Fig. 3, for solutes Ti, V, and Zr, both elastic and electronic interactions become more repulsive when the supercell changes from 108-atoms to 64-atoms. Therefore, the repulsive interactions of these solutes with vacancy are higher, estimated by using 64-atom supercell. For the solutes Ge and Sn, their elastic binding energy values decrease while the electronic binding energy values increase when we lower the supercell size, *i.e.*, the number of atoms contained in a supercell is reduced from 108 to 64. As a result, the changes of elastic and electronic binding energies offset each other to some extent. Thus, the total binding energies of solutes Ge and Sn with the vacancy are insensitive to the change of supercell size.

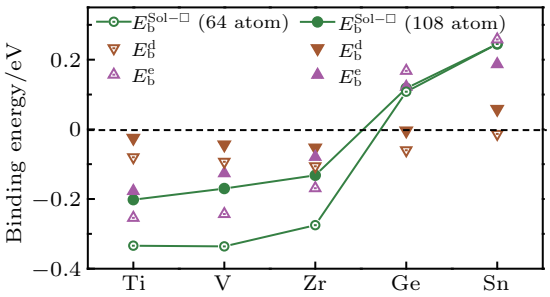


Fig. 3. Comparison of overall solute–□ binding energy $E_{\rm b}^{\rm Sol-\square}$, the distortion binding energy ($E_{\rm b}^{\rm d}$), and electronic binding energy ($E_{\rm b}^{\rm e}$) between supercell sizes containing108 atoms and 64 atoms.

Figure 4 shows the calculated results of elastic and elec-

tronic binding energies as a function of atomic number. Overall, the elastic interaction energy is smaller than the electronic energy for each of these 3d, 4p, 4d, 5p solutes, and the variation of each total binding energy follows a similar trend to the variation trend of its corresponding electronic energy, which suggests that the electronic effect plays a major role in the solute–□ interaction. Particularly, for the solute elements in the middle, the electronic effect and elastic effect compete with each other.

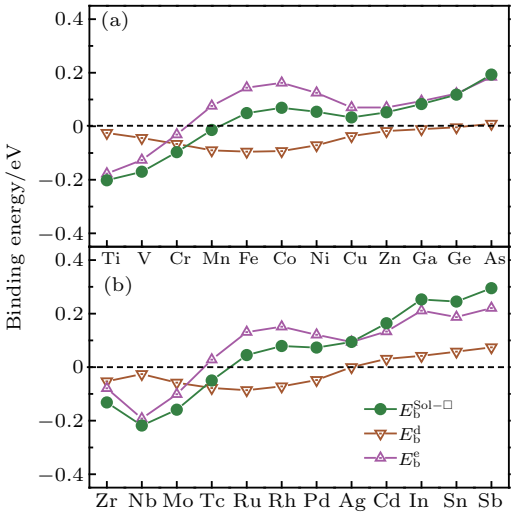


Fig. 4. Variations of distortion binding energy (E_b^d) and electronic binding energy (E_b^e), decomposed from total solute–□ binding energy $E_b^{Sol-□}$, with atom numbers.

As far as the elastic interaction is concerned, it is suggested that undersized (oversized) solutes, *i.e.*, those solute atoms with smaller (larger) atomic volume than the host atoms, cause the lattices to contract (expand), whereas the vacancies lead the lattices to shrink.[26,27] The addition of solute elements with different lattice constants will result in lattice-mismatching-induced strain, and thus raising the energy of the host.[28] However, the internal strain may be cancelled to a certain extent by the association of the oversized solute and vacancy. Therefore, the vacancy will be attractive to the oversized solute and repulsive to the undersized solute. These are confirmed by our calculations. Figure 5 shows the results of solute volume of the 3d, 4p, 4d, 5p solutes in Al, which are calculated from

$$V_{\mathrm{Sol}} = V_{\mathrm{cont-sol}} - V_{\mathrm{tot}}, \tag{5}$$

where $V_{\mathrm{cont-sol}}$ and V_{tot} are the volume of the supercell with and without a single solute atom, respectively. Positive and negative values mean the expansion and contraction of the lattice. Meanwhile, the atomic volumes of these elements are also shown in Fig. 5 for comparison. It can be clearly seen that the elements at the beginning and in the end with larger atomic volume Ω have positive solute volume V_{sol} while the solutes in the middle with low Ω have negative V_{sol}.

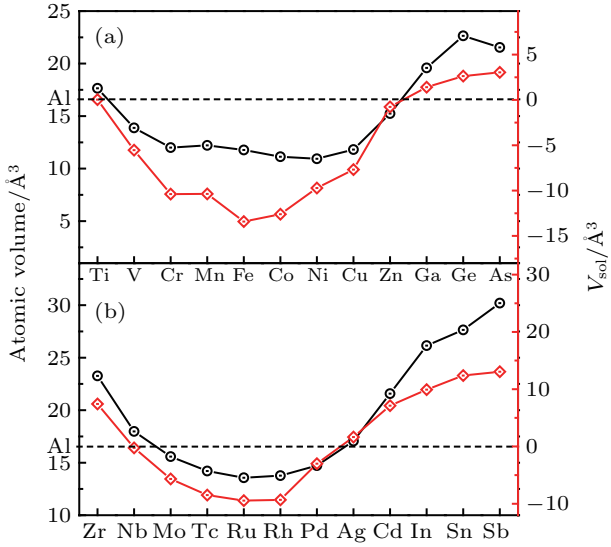


Fig. 5. Variations of atomic volume Ω and solute volume V_{sol} of (a) 3d–4p; (b) 4d–5p solutes with atom number.

Figure 6 shows the dependence of the solute–□ elastic binding energy on solute volume. An evident positive linear correlation is observed between the elastic binding energy and the solute volume. The elastic binding energy increases as the value of V_{sol} increases. The elastic interaction is repulsive for the undersized solute but attractive for the oversized solute. The only exception is solute Zr, whose underlying physics needs further studying.

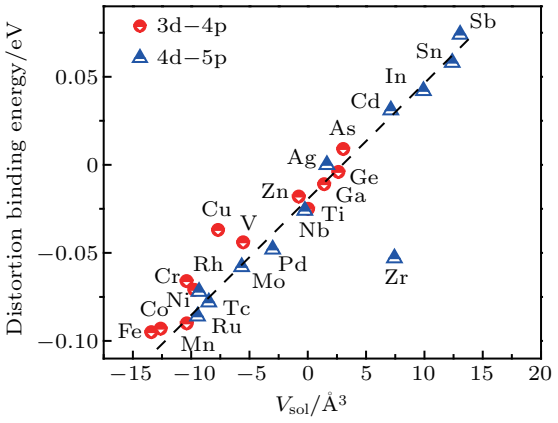


Fig. 6. Variations of distortion binding energy with solute volume, for 3d–4p and 4d–5p.

The electronic effect is encompassed in the electron redistribution. The differential charge density for solute–□ binding is calculated in the cases of Nb, Cu, and Sb. As shown in Fig. 7, there is no obvious charge transfer between the solute and vacancy for the element Cu, indicating a very weak electronic interaction. An obvious electron charge shift can be observed from the vacancy region to the solute atoms in the case of solute Sb, showing a strong electronic attraction, whereas the electron charge shifts from the solute towards the opposite direction of the vacancy region for solute Nb with a strong electronic repulsion.

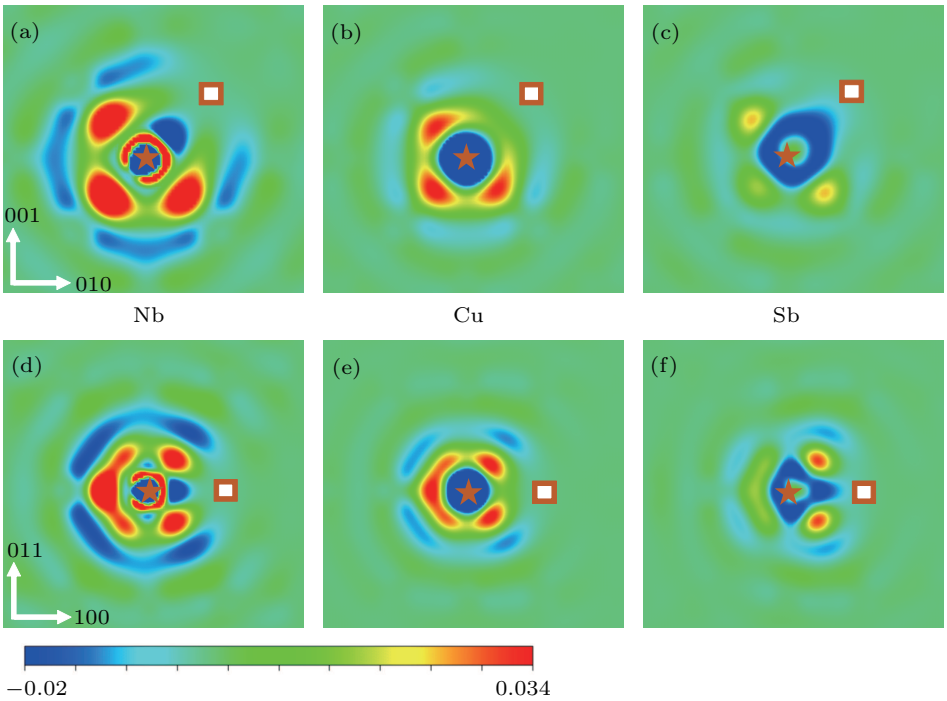


Fig. 7. Differential charge density map for the solute–□ pair in the (1 0 0) and (0 1 −1) plane. Brown (gray in black/white) star and square denote solute atom and the vacancy, respectively, for [(a) and (d)] solute atom Nb, [(b) and (e)] solute atom Cu, and [(c) and (f)] solute atom Sb. Unit is $e/Å^3$.

4. Conclusions

In this work, systematic first principles calculations are carried out to investigate the 3d, 4p, 4d, 5p solute–□ interactions in fcc Al. The solute–□ interactions gradually transform from repulsion to attraction from left to right for the 3d–4p and 4d–5p series. The evolution trend is consistent well with the variation trends of previous theoretical results. The energy values for the late elements show high consistency whereas noticeable discrepancies are observed for the initial elements, which arises from the difference in supercell size. The origin of the solute–□ binding energy behaviors is discussed from the viewpoints of the elastic interaction and electronic interaction. Overall, the variation of electronic binding energy follows a similar trend as that of the total binding energy and plays a major role in the solute–□ interaction. The elastic interaction of the solute–□ pair is repulsive for the undersized solutes but attractive for the oversized solutes. The elastic binding energy is linearly related to the solute volume.

References

[1] Gayle F M and Goodway M 1994 *Science* **266** 1015
[2] Ohta M, Hashimoto F and Tanimoto T 1968 *Memoirs of the School of Engineering* (Okayama: Okayama University) pp. 39–50
[3] Ohta M and Hashimoto F 1965 *Trans. Jpn. Inst. Met.* **6** 9
[4] Raman K, Das E and Vasu K 1971 *J. Mater. Sci.* **6** 1367
[5] Melikhova O, Kuriplach J, Čížek J and Procházka I 2006 *Appl. Surf. Sci.* **252** 3285
[6] Balluffi R W and Ho P S 1973 *Diffusion* (Metal Park, OH: American Society for Metals) p. 83
[7] Wolverton C 2007 *Acta Mater.* **55** 5867
[8] Simonovic D and Sluiter M H 2009 *Phys. Rev. B* **79** 054304
[9] Hoshino T, Zeller R and Dederichs P 1996 *Phys. Rev. B* **53** 8971
[10] Ohnuma T, Soneda N and Iwasawa M 2009 *Acta Mater.* **57** 5947
[11] You Y W, Kong X S, Wu X B, Liu W, Liu C S, Fang Q, Chen J, Luo G N and Wang Z 2014 *J. Nucl. Mater.* **455** 68
[12] Kong X S, Wu X B, You Y W, Liu C S, Fang Q, Chen J L, Luo G N and Wang Z 2014 *Acta Mater.* **66** 172
[13] Shin D and Wolverton C 2010 *Acta Mater.* **58** 531
[14] Perdew J P, Burke K and Ernzerhof M 1996 *Phys. Rev. Lett.* **77** 3865
[15] Kresse G and Furthmüller J 1996 *Comput. Mater. Sci.* **6** 15
[16] Kresse G and Furthmüller J 1996 *Phys. Rev. B* **54** 11169
[17] Blöchl P E 1994 *Phys. Rev. B* **50** 17953
[18] Kresse G and Joubert D 1999 *Phys. L Rev. B* **59** 1758
[19] Monkhorst H J and Pack J D 1976 *Phys. Rev. B* **13** 5188
[20] Eisenmann B and Schäfer H 1988 *Structure Data of Elements and Intermetallic Phases* (Berlin: Springer-Verlag)
[21] Every A and McCurdy A 1992 *Low Frequency Properties of Dielectric Crystals* (Berlin: Springer-Verlag)
[22] Bass J 1967 *Philos. Mag.* **15** 717
[23] Kurth S, Perdew J P and Blaha P 1999 *Int. J. Quantum Chem.* **75** 889
[24] Stampfl C and Van de Walle C 1999 *Phys. Rev. B* **59** 5521
[25] Carling K, Wahnström G, Mattsson T R, Mattsson A E, Sandberg N and Grimvall G 2000 *Phys. Rev. Lett.* **85** 3862
[26] Olsson P, Klaver T and Domain C 2010 *Phys. Rev. B* **81** 054102
[27] Li Y J, Kulkova S E, Hu Q M, Bazhanov D I, Xu D S, Hao Y L and Yang R 2007 *Phys. Rev. B* **76** 064110
[28] Lin K and Zhao Y P 2019 *Extreme Mech. Lett.* **30** 100501